Clinical Neurophysiology 140 (2022) 98–109

Contents lists available at ScienceDirect

Clinical Neurophysiology

journal homepage: www.elsevier.com/locate/clinph

The influence of sensory potentials on transcranial magnetic stimulation – Electroencephalography recordings

Nahian S. Chowdhury [a,b,*], Nigel C. Rogasch [c,d,e], Alan K.I. Chiang [a], Samantha K. Millard [a,b], Patrick Skippen [a], Wei-Ju Chang [a], Katarzyna Bilska [a,b], Emily Si [a], David A. Seminowicz [f,g], Siobhan M. Schabrun [a]

[a] *Center for Pain IMPACT, Neuroscience Research Australia, Sydney, New South Wales, Australia*
[b] *University of New South Wales, Sydney, New South Wales, Australia*
[c] *Discipline of Psychiatry, Adelaide Medical School, University of Adelaide, Adelaide, South Australia, Australia*
[d] *Hopwood Centre for Neurobiology, Lifelong Health Theme, South Australian Health and Medical Research Institute, Adelaide, South Australia, Australia*
[e] *Turner Institute for Brain and Mental Health, School of Psychological Sciences and Monash Biomedical Imaging, Monash University, Melbourne, Victoria, Australia*
[f] *Department of Neural and Pain Sciences, University of Maryland School of Dentistry, Baltimore, MD, 21201, United States*
[g] *Center to Advance Chronic Pain Research, University of Maryland Baltimore, Baltimore, MD 21201, United States*

A R T I C L E I N F O

Article history:
Accepted 26 May 2022
Available online 11 June 2022

Keywords:
Transcranial magnetic stimulation
Electroencephalography
TMS-EEG
Sham stimulation
Sensory-evoked potentials

H I G H L I G H T S

- Sensory-evoked activity can contaminate TMS-evoked potentials (TEPs).
- A spatially matched sensory sham showed contamination of TEPs > 55 ms post-stimulation.
- Contamination was not explained by a linear sum of auditory and somatosensory stimulation alone.

A B S T R A C T

Objective: It remains unclear to what extent Transcranial Magnetic Stimulation-evoked potentials (TEPs) reflect sensory (auditory and somatosensory) potentials as opposed to cortical excitability. The present study aimed to determine; a) the extent to which sensory potentials contaminate TEPs using a spatially-matched sham condition, and b) whether sensory potentials reflect auditory or somatosensory potentials alone, or a combination of the two.
Methods: Twenty healthy participants received active or sham stimulation, with the latter consisting a sham coil click combined with scalp electrical stimulation. Two additional conditions i) electrical stimulation and ii) auditory stimulation alone, were included in a subset of 13 participants.
Results: Signals from active and sham stimulation were correlated in spatial and temporal domains > 55 ms post-stimulation. Relative to auditory or electrical stimulation alone, sham stimulation resulted in a) larger potentials, b) stronger correlations with active stimulation and c) a signal that was not a linear sum of electrical and auditory stimulation alone.
Conclusions: Sensory potentials can confound interpretations of TEPs at timepoints > 55 ms post-stimulation. Furthermore, TEP contamination cannot be explained by auditory or somatosensory potentials alone, but instead reflects a non-linear interaction between both.
Significance: Future studies may benefit from controlling for sensory contamination using spatially-matched sham conditions, and which consist of combined auditory and somatosensory stimulation.
© 2022 International Federation of Clinical Neurophysiology. Published by Elsevier B.V. All rights reserved.

1. Introduction

Transcranial magnetic stimulation (TMS) produces evoked potentials (TEPs) during electroencephalography (EEG) that can index cortical excitability (Farzan et al., 2016; Ilmoniemi and Kičić, 2010; Tremblay et al., 2019). While traditional assessment of excitability involves TMS delivered to motor cortex with output

* Corresponding author at: Neuroscience Research Australia, 139 Barker Street, Randwick 2031, NSW, Australia.
E-mail address: n.chowdhury@neura.edu.au (N.S. Chowdhury).

https://doi.org/10.1016/j.clinph.2022.05.015
1388-2457/© 2022 International Federation of Clinical Neurophysiology. Published by Elsevier B.V. All rights reserved.

measured from peripheral muscles, TMS-EEG permits assessment of cortical excitability not confounded by spinal/peripheral excitability, and assessment of excitability from non-motor regions (Farzan et al., 2016). Although TMS-EEG holds promise in exploring functional brain activity and connectivity in both healthy and clinical populations, TEPs can be contaminated by sensory input arising from the TMS pulse, confounding data interpretation.

Two kinds of sensory-evoked potentials may contribute to TEPs: auditory potentials elicited by the "clicking" of the TMS coil, and somatosensory potentials elicited by the "flicking" sensation on the skin. Several masking methods have been used to suppress these sensory inputs. For example, white noise played through headphones has been used to mask the click sound (Ilmoniemi and Kičić, 2010; Kičić, 2009), while a thin layer of foam placed between the TMS coil and EEG cap has been used to minimize the scalp sensation (Massimini et al., 2005). However, recent studies have shown that even when these methods are used, sensory contamination of TEPs is still present (Biabani et al., 2019; Conde et al., 2019; Rocchi et al., 2021). Specifically, TMS produced similar signals to sham conditions that mimicked the auditory and/or somatosensory aspects of active TMS (e.g., scalp electrical stimulation with a TMS click away from the scalp). This suggests masking may not be sufficient to prevent sensory contamination, leading authors (Biabani et al., 2019; Conde et al., 2019) to recommend the use of sham conditions to control for sensory contamination.

One limitation of previous sham conditions is the sensory components were not spatially matched to active TMS. For example, four studies induced auditory potentials by delivering active TMS at a distance from the scalp, and concurrently administered mild scalp electrical stimulation to induce somatosensory potentials (Conde et al., 2019; Fernandez et al., 2021; Gordon et al., 2018; Gordon et al., 2021), while another study used a sham condition where active TMS was delivered to the shoulder (Biabani et al., 2019). These studies typically demonstrated sensory contamination between ~60–250 ms post-stimulation, with earlier timepoints (<60 ms) less impacted by sensory contamination (Biabani et al., 2019; Gordon et al., 2018; Poorganji et al., 2021; Rocchi et al., 2021). However, the use of sham conditions that do not induce auditory or somatosensory potentials that are spatially matched to active TMS may underestimate the degree of sensory contamination.

Another unaddressed question is the extent to which contamination of TEPs is explained by auditory or somatosensory potentials, or a combination of both. A study by Rocchi and colleagues (Rocchi et al., 2021) showed somatosensory contributions to TEPs were significantly smaller than auditory contributions, with auditory stimulation alone generating similar signals to active TMS ~100–200 ms after the TMS pulse. The authors concluded sensory contamination of TEPs is explained mostly by auditory potentials and controlling for these alone may be sufficient to index excitability. However, the authors did not assess the combined effects of auditory and somatosensory stimulation, as occurs in active TMS. While somatosensory contributions to TEPs are smaller than auditory contributions, the combination of these may result in evoked potentials that more strongly resemble the sensory potentials produced by active TMS. Indeed, several studies have shown that when two sensory stimuli are presented simultaneously, the resultant neural response is larger than the sum of the responses to the respective unisensory stimuli (Senkowski et al., 2007). This non-linear interaction has been demonstrated in rat studies using somatosensory and visual stimuli (Lippert et al., 2013; Nikbakht et al., 2018), human fMRI studies using visual and auditory stimuli (Calvert et al., 2000; Calvert et al., 2001), and human EEG studies using somatosensory and auditory stimuli (Ronga et al., 2021). If this occurs in active TMS, sham conditions consisting of auditory input alone will not be sufficient to control for sensory contamination of the TEP.

The present study had two aims. The first was to determine whether similar contamination of TEPs would be observed to previous studies (Biabani et al., 2019; Gordon et al., 2018; Poorganji et al., 2021; Rocchi et al., 2021) when using a spatially matched sham condition. The sham stimuli consisted of concurrent scalp electrical and auditory stimulation (sham coil click) over the left primary motor cortex, delivered at the same location as active TMS. The second aim was to determine the degree of TEP contamination explained by auditory or somatosensory potentials alone and in combination. This aim was addressed by including two control conditions (electrical and auditory stimulation alone) in a subsample of participants. The combination of auditory and electrical stimulation was hypothesised to produce a) larger evoked potentials, b) stronger contamination of TEPs and c) a signal that could not be explained by a linear sum of the responses from electrical or auditory stimulation alone.

2. Methods

2.1. Participants

20 healthy participants (13 males, 7 females, 16 TMS- naïve, age; 28.1 ± 5.3). Participants completed a TMS safety screen (Rossi et al., 2009). Participants were excluded if they were pregnant, reported a history of neurological or psychiatric conditions, or were taking psychoactive medication. Procedures adhered to the Declaration of Helsinki and were approved by the human research ethics committee of UNSW (HC200328). All participants provided informed written consent.

2.2. Experimental protocol

Fig. 1 shows the protocol. Participants were seated comfortably in a shielded room. They viewed a fixation cross to minimise eye movements and did not observe changes in the setup between conditions. Participants wore both foam earplugs and headphones to reduce any potential discomfort from, and to dampen the noise from, the TMS click. Masking noise was not played through the headphones as the aim was for participants to perceive the TMS click to compare loudness ratings between conditions. The active and sham TMS coils were covered in a layer of foam (5 mm thickness) to minimize any sensations related to coil vibration (Massimini et al., 2005).

The experiment consisted of a single session in which participants experienced multiple blocks of TMS pulses (in randomized order), each consisting of ~60 trials. All 20 participants received one block of 1) real stimulation over M1 (active condition) and 2) concurrent scalp electrical stimulation and a sham coil click, with both delivered over the same location as the active condition (sham condition). Inclusion of these conditions addressed the first aim of the study, which was to assess sensory contamination of TEPs using a spatially-matched sham condition. A subsample of the participants (Participants 8–20) received two additional blocks of 3) electrical stimulation applied over M1 (electric condition), and 4) auditory stimulation (sham coil click) applied over M1 (auditory condition). Inclusion of these conditions addressed the second aim of the study, which was to determine the degree of TEP contamination explained by auditory or somatosensory potentials alone and in combination.

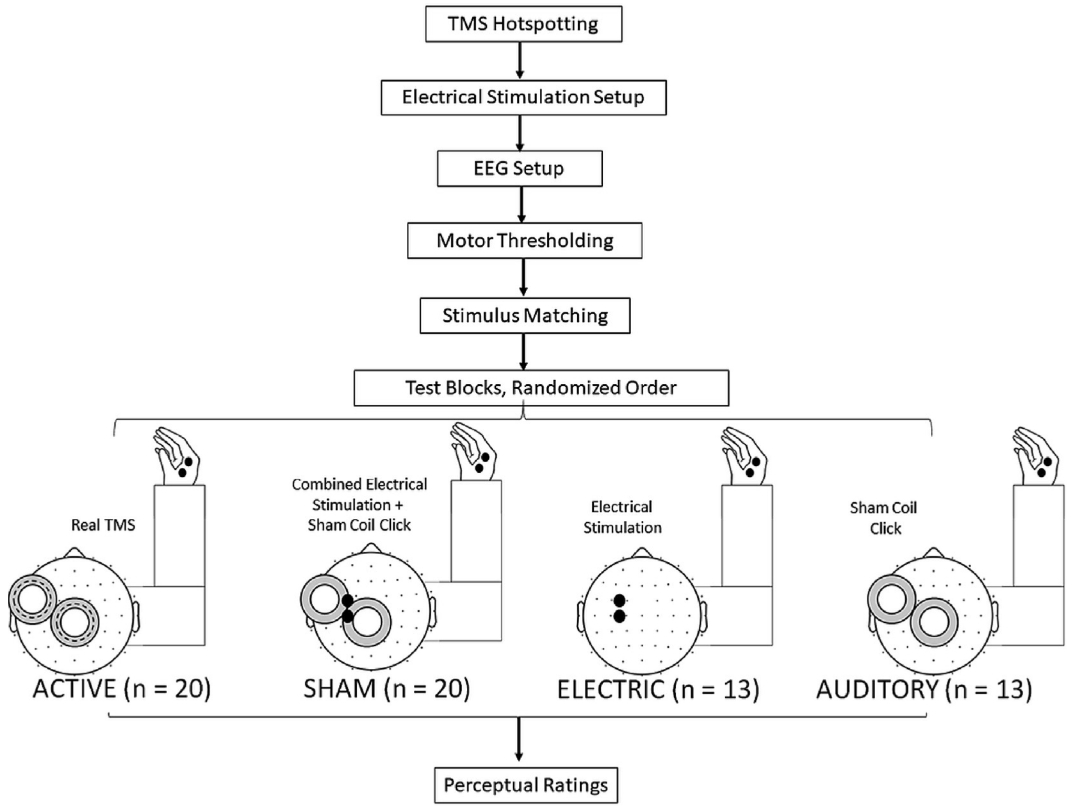

Fig. 1. Schematic of the experimental protocol.

2.3. TMS hotspotting

Surface electromyography (EMG) over the right first dorsal interosseous (FDI) muscle was used to record motor-evoked potentials (MEPs). EMG (8 mm Ag/AgCl electrode) was recorded using NeuroMEP (Neurosoft, Russia) sampled at 2 kHz. A mains filter of 50 Hz was applied, with a low and high pass filter at 1000 and 10 Hz respectively. Single, biphasic stimuli were delivered to left primary motor cortex using a Magstim Super Rapid^2 Plus and a 70 mm figure-of-eight air cooled coil (Magstim Ltd., UK). The coil was oriented at 45° to the midline, inducing a current in the posterior-anterior direction. The scalp site that evoked the largest MEP measured at the FDI ('hotspot') was determined. This location was marked and informed the location of scalp electrical stimulation.

2.4. Electrical stimulation

Prior to EEG setup, 8 mm Ag/AgCl electrodes were placed directly over the scalp. "Snap on" lead wires were then clipped in place and connected to the electrical stimulator (Digitimer DS7AH, Digitimer Ltd., UK). To keep the electrodes and lead wires firmly in position, participants were fitted with a tight netted wig cap, which sat on top of the electrodes but underneath the EEG cap. Consistent with previous research (Rocchi et al., 2021), and to minimize EEG artefacts caused by electrical stimulation, the stimulating electrodes were not placed directly underneath the EEG electrodes. Rather, stimulating electrodes were positioned in the middle of the EEG electrode cluster located in closest proximity to the motor hotspot. This roughly corresponded to an anode position between FC1 and FC3 and a cathode position between C1 and C3. Scalp electrical stimulation was delivered using a 200 μs square wave with a compliance of 200 V.

2.5. Electroencephalography

EEG was recorded using a DC-coupled, TMS-compatible amplifier (ActiChamp Plus, Brain Products, Germany) at a sampling rate of 25000 Hz. Signals were recorded from 63 active electrodes, embedded in an elastic cap (ActiCap, Brain Products, Germany), in line with the 10–10 system. Active electrodes result in similar TEPs (both magnitude and peaks) to more commonly used passive electrodes (Mancuso et al., 2021). Recordings were referenced online to 'FCz' and the ground electrode placed on 'FPz'. Electrolyte gel was used to reduce electrode impedances below ~ 5kOhms.

2.6. Motor thresholding

TMS was delivered over the location of the stimulation electrodes. The resting motor threshold (RMT) was determined using the TMS motor thresholding assessment tool, which estimates the lowest TMS intensity required to reliably induce an MEP (Awiszus and Borckardt, 2011), with the MEP amplitude threshold set at 50 microvolts (Rossini et al., 1994; Rothwell et al., 1999). The test stimulus intensity was set at 110% RMT.

2.7. Stimulus matching

As the aim was to perceptually match the somatosensory aspects of active and sham TMS, a 2-Alternative Forced Choice task was used to determine the electrical stimulation intensity that led to a similar flicking sensation to active TMS. Participants received either electrical stimulation or active TMS in a randomized order and were asked whether the first or second stimulus led to a stronger flick sensation. The electrical stimulation intensity was then increased or decreased until participants could no longer judge the first or second stimulus as stronger. This intensity was then applied during the test blocks.

2.8. Test blocks

Test blocks occurred in a randomly determined order, each consisting of $\sim$ 60 pulses that were delivered manually from the machine. A test–retest reliability study by Kerwin et al., (2018) showed that 60 TMS pulses (delivered in the same run) was sufficient to obtain within-individual concordance between the resultant TEP peaks of each trial. All 20 participants received a single block of both active and sham stimulation. For the sham condition, an air-cooled sham coil (Magstim Ltd., UK) was simultaneously triggered with the electrical stimulation unit. The sham coil induces a small magnetic field without inducing brain current, while retaining the click sound associated with the active coil. Although some sham coils have been shown to produce small cortical electrical fields (Smith and Peterchev, 2018), the sham coil used in our study was delivered at a distance from the scalp due to the presence of an EEG cap, electrical stimulation setup, and foam placed over the coil, making it unlikely that the sham coil induced cortical activation. Piloting using perceptual ratings revealed a sham stimulus intensity of 100% was required to match the loudness of the sham click as closely as possible to the active TMS click. As such, this intensity was used in the sham TMS blocks. For 13 out of the 20 participants, 2 additional blocks were included consisting of electrical or auditory (sham coil click) stimulation alone.

2.9. Perceptual ratings

After each block, participants were asked to rate how loud the TMS click was (0 = I did not hear anything, 10 = I heard an extremely loud click), how strong the flick sensation was (0 = I felt nothing, 10 = I felt an extremely hard flick), how sharp the flick was if it was felt (0 = the flick was extremely broad, 10 = the flick was extremely narrow), how tolerable the TMS was (0 = very intolerable, 10 = very tolerable) and the extent to which they thought the brain area underneath the coil was being stimulated (0 = the brain was not stimulated at all, 10 = the brain was very much stimulated).

2.10. Pre-processing

Pre-processing of the data was completed using EEGLAB (Delorme and Makeig, 2004) and TESA (Rogasch et al., 2017) in MATLAB (R2020b, The Math works, USA), and based on previously described methods (Mutanen et al., 2020; Mutanen et al., 2018; Rogasch et al., 2017). First, bad channels were removed. The number of channels removed across participants was 2.47 ± 2.3. The period between −5 and 8.6 ms (±1.83) after the TMS pulse was removed and interpolated using the ARFIT function for continuous data (Neumaier and Schneider, 2001; Schneider and Neumaier, 2001). The exact interval was based on the duration of decay artefacts. Data was epoched 1000 ms before and after the TMS pulse, and baseline corrected between −1000 and −5ms before the TMS pulse. Noisy epochs were identified via the EEGLAB auto-trial rejection function (Delorme et al. 2007) and then visually confirmed. The number of epochs excluded was 1.22 ± 2.65, 1.83 ± 2.9, 0.75 ± 1.21 and 0.83 ± 1.4 for the active, sham, electric and auditory conditions respectively. The source-estimation noise-discarding (SOUND) algorithm was applied (Mutanen et al., 2020; Mutanen et al., 2018), which estimates and supresses noise at each channel based on the most likely cortical current distribution given the recording of other channels. This signal was then re-referenced (to average). A band-pass (1–100 Hz) and band-stop (48–52 Hz) Butterworth filter was then applied. Any lost channels were interpolated. Similar to a previous study comparing active and sham TMS (Conde et al., 2019), we did not use ICA in the pre-processing pipeline. ICA has been shown to introduce artificial correlations between active and sham TMS in the baseline period (Biabani et al., 2019). ICA may also remove common sensory components that may not be identified in the correlation analysis. Furthermore, a recent study (Rogasch et al., 2022) comparing TMS-EEG pre-processing pipelines argued for the use of the simplest pipeline, and that aggressive approaches such as ICA should only be used if necessary. Nonetheless, the results of the analysis when using the fastICA algorithm with auto-component rejection (Rogasch et al., 2017) before the SOUND pre-processing step are shown in the Supplementary Material for comparison.

2.11. Statistical analysis

2.11.1. Perceptual ratings

JASP software (Version 0.12.2.0, JASP Team, 2020) was used to conduct Bayes paired samples t-tests (Cauchy scale = 0.707), comparing the active and sham conditions on ratings of perceived loudness, flick strength, flick sharpness, tolerability, and stimulation extent. To determine whether combined electrical and auditory stimulation enhanced the experience of “real” brain stimulation, stimulation extent in the sham condition was compared against the auditory and electric conditions. Bayes factors were expressed as BF_{10} values, where a value <=0.33 indicated evidence that the perceptual ratings were matched between conditions (Stefan et al., 2019).

2.11.2. Aim 1: Sensory contributions to TEPs

The grand-averaged signals and global mean field waveform (GMFW: standard deviation across electrodes over time, averaged across trials (Rogasch et al., 2017)) were obtained for active and sham stimulation. Maxima in the GMFW were identified using the TESA peak function (Rogasch et al., 2017). In line with previous studies (Conde et al., 2019; Rocchi et al., 2021), based on the peaks of the GMFW of the active condition, signals were separated into early, mid and late time-points of interest (TOIs) (Conde et al., 2019; Rocchi et al., 2021). The Fieldtrip toolbox (Oostenveld et al., 2011) was used to conduct a cluster-based permutation analysis to compare amplitude levels between active and sham conditions at each TOI. We determined the spatial correlation between the active and sham conditions. The spatial correlation examines the extent to which the scalp (topographical) distribution of the signal is similar between the active and sham conditions. Specifically, at each timepoint, the spearman-ranked correlation in signal amplitude was calculated between the active electrodes (Active_{E1}, Active_{E2}, ... Active_{E63}) and sham electrodes (Sham_{E1}, Sham_{E2}, ... Sham_{E63}), where “Active_{Ex}” or “Sham_{Ex}” represents the signal amplitude at one of the 63 electrodes (E). We also determined the temporal correlation between the active and sham conditions. The temporal correlation examines the extent to which fluctuations in voltage across time are similar under the active and sham conditions. Specifically, at each electrode, the spearman-ranked correlation was calculated between the signal amplitude of the active signal (Active_{T1}, Active_{T2}, ... Active_{Tn}) and the signal amplitude of the sham signal (Sham_{T1}, Sham_{T2}, ... Sham_{Tn}), where “Active_{Tx}” or “Sham_{Tx}” represents signal amplitude at one of the timepoints (T) in the time window (T1-Tn). Correlation coefficients were transformed using Fisher’s z method. For spatial correlations, the 95% confidence interval of the mean correlation value (across participants) at each time-point was assessed against zero (Biabani et al., 2019). Temporal correlations were performed separately for early, mid and late TOIs. The mean correlation value (across participants) at each electrode was assessed against zero (Biabani et al., 2019). Lastly, to determine whether the GMFW maxima in the active condition were retained after controlling for sensory-evoked potentials, signal-space projection with source-informed reconstruction (SSP-SIR) (Biabani et al., 2019) was used to suppress sensory potentials observed in the sham condition from the active condition. SSP-SIR is a filter which identifies spatial commonalities between two signals and suppresses this from the target signal.

2.11.3. Aim 2: Individual sensory contributions to TEPs

The grand-averaged signal and GMFW were obtained for active, sham, electrical and auditory stimulation, and the spatial and temporal correlations between conditions were computed. To determine whether the combination of auditory and electrical stimulation generated stronger sensory-evoked potentials compared to each condition alone, a cluster-based permutation analysis was conducted comparing the sham condition with the electric and auditory conditions. To determine whether there were stronger correlations with active TMS when electrical and auditory stimulation was combined (sham) vs. delivered alone (electric or auditory), the spatial correlations for active-sham were compared with active-electric and active-auditory. This was done by running a two-sample t-test comparing the mean z-transformed correlation coefficients (across participants) at each time-point. Lastly, to assess whether a simple linear summation of somatosensory and auditory-evoked potentials could capture the responses observed in the sham, the responses from the electric and auditory condition were added, and spatial and temporal correlations between the summed signal and the sham signal were determined.

3. Results

Two participants were excluded due to evidence of bridging across electrodes but were included in the analysis of perceptual ratings. This left 18 participants relevant to the first aim of the study, and 12 participants relevant to the second aim. Note these sample sizes remained comparable with previous studies investigating sham conditions, which ranged from 12-20 (Biabani et al., 2019; Conde et al., 2019; Gordon et al., 2018; Rocchi et al., 2021). The mean RMT and test stimulus intensity was 84 ± 9% and 91 ± 9% of maximum stimulator output respectively. While the mean RMT was relatively higher than previous studies using biphasic TMS during EEG (Casula et al., 2018; Sekiguchi et al., 2011), this can be explained by additional aspects of the set-up protocol that increased the distance between the coil and the scalp, including the stimulation electrodes and leads, wig cap, and layer of coil foam. The mean test electrical stimulation intensity was 5. 5 ± 8.1 mA. This intensity is comparable to previous studies using sham electrical stimulation (Conde et al., 2019; Rocchi et al., 2021) and is insufficient to directly activate the cortex (Arana et al., 2008; Conde et al., 2019; Rocchi et al., 2021). The average interpulse interval was 2.5 seconds.

3.1. Perceptual ratings

Fig. 2 shows the perceptual ratings for each condition. There was no significant difference between active and sham conditions in click loudness, (p = 0.07, BF_{10} = 0.97), flick strength, (p = 0.35, BF_{10} = 0.33), flick sharpness, (p = 0.6, BF_{10} = 0.26) and tolerability, (p = 0.34, BF_{10} = 0.34). As the Bayes factors yielded inconclusive support for the matching of loudness between active and sham, a Bayesian t-test comparing loudness ratings in active and auditory conditions was conducted (n = 13). This was justified given an identical sham coil click was used in the auditory and sham conditions. This analysis yielded a BF_{10} value of 0.302, suggesting the click of the sham coil and active TMS were matched in terms of loudness. Participants rated active TMS as stimulating the brain to a larger extent than sham (p = 0.01, BF_{10} = 3.7). Stimulation extent was rated higher in the sham compared to either auditory (p <.001, BF_{10} = 69.5) or electrical stimulation alone (p <.001, BF_{10} = 782.3), suggesting the combination of auditory and electrical stimulation enhances the experience of "real" stimulation.

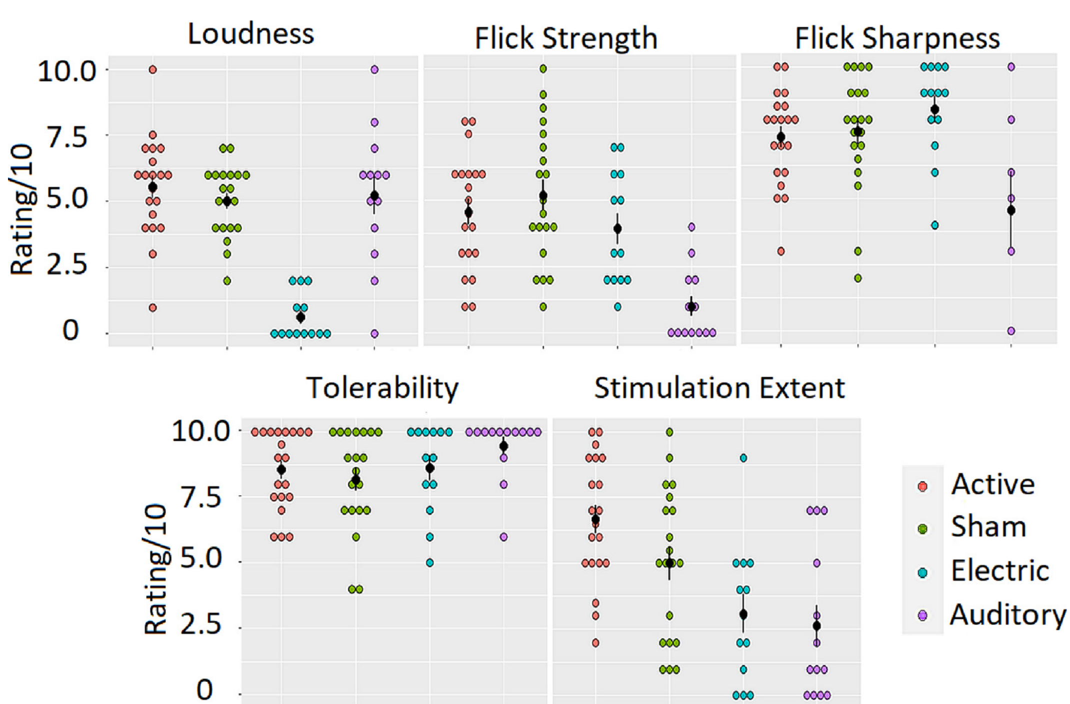

Fig. 2. Dotplots showing participant ratings of Transcranial Magnetic Stimulation (TMS) click loudness, flick strength, flick sharpness (rated only if a flick was felt), tolerability and stimulation extent (i.e., perceived extent to which brain area underneath the coil was being stimulated).

3.2. Sensory contributions to TMS-evoked potentials

Four maxima were identified in the active condition, including 16, 44, 89 and 175 ms after TMS (Fig. 3). Based on the peaks of the GMFW, three TOIs were selected for comparison between the active and sham conditions– early (12–55 ms), middle (56–135 ms) and late (136–250 ms) time periods. Cluster-based permutation analysis was used to compare signal amplitude at each of the 3 TOIs. At the early TOI, there was a significantly stronger positive amplitude in the active vs. the sham condition in occipital sites ($p = .049$) and a significantly stronger negative amplitude in the active vs. the sham condition in left frontal ($p = 0.008$) and right frontocentral sites ($p = .04$). For the suppressed signal (after SSP-SIR), the GMFW was substantially attenuated relative to active stimulation (Fig. 3). However, all four maxima were retained. Grand-averages and scalp topographies for the active, sham, and suppressed signals for the full sample of 18, are shown in Fig. 4.

Significant positive spatial correlations between the active and sham conditions were present at mid and late TOIs, but not the early TOI (Fig. 5). This suggests that the topographical distribution of the signal was similar between the active and sham conditions at timepoints > 55 ms post-stimulation. Significant positive temporal correlations were present at the early (right-occipital), middle (global) and late (global) TOIs (Fig. 5), suggesting that > 55 ms post-stimulation, fluctuations in voltage across time were similar between the active and sham conditions across scalp regions. Together these findings suggest the active and sham signals were correlated in both spatial and temporal domains at timepoints > 55 ms post-stimulation.

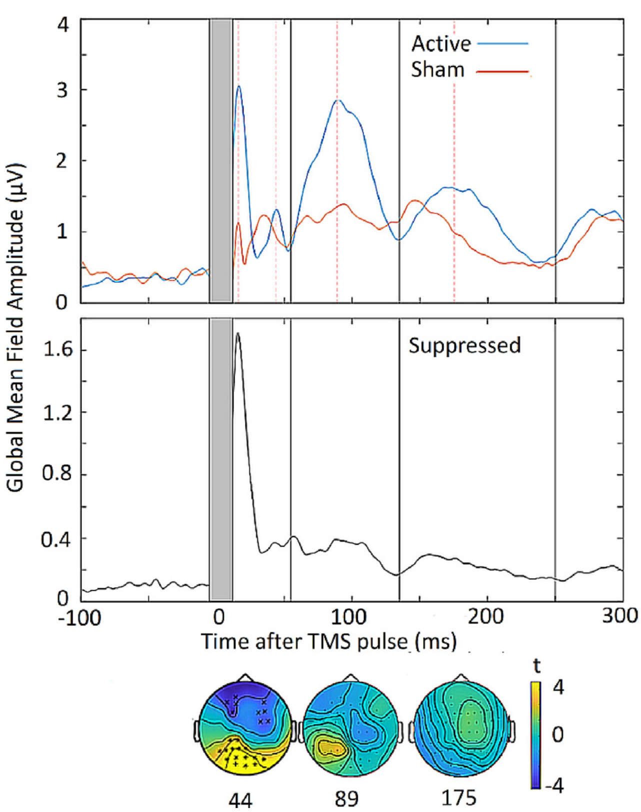

Fig. 3. ***Active stimulation produces a larger signal than sham stimulation.*** The figure shows the amplitude comparisons between the active and sham conditions. The top panel shows the global mean field waveform (GMFW) for the active and sham conditions. The black solid lines represent the boundaries of the time points of interest (TOI) – early (12–55 ms), mid (56–135 ms) and late (136–250 ms), and red-dotted lines show the maxima of the active signal. The middle panel shows the GMFW for the suppressed signal (i.e., the resultant signal when spatial commonalities between the active and sham signal were removed). The bottom panel shows the cluster plots comparing signal amplitude between the active and sham conditions at a representative timepoint at each TOI (early-44 ms, mid-89 ms, late-175 ms). The black stars demonstrate the presence of significant positive (yellow) or negative (blue) clusters.

3.3. Individual sensory contributions to TMS-evoked potentials

Grand-averages and scalp topographies for the active, sham, electric and auditory conditions for the subsample of 12 are shown in Fig. 6.

The active and sham correlations (Fig. 7) largely corresponded to the full sample, with significant positive spatial correlations at TOIs > 55 ms, and similarly distributed positive temporal correlations at all TOIs (Fig. 7A). There were significant positive spatial and temporal correlations between the active and electric conditions at late TOIs (Fig. 7B). When comparing the electric to the sham condition, there were significant temporal and spatial correlations at all TOIs, though these were more frequently observed at early and mid TOIs (Fig. 7B). There were significant positive temporal correlations between active and auditory conditions at early (right-parietal), middle (frontal and central-occipital) and late (frontal and temporal) TOIs, and significant positive spatial correlations at mid and late TOIs (Fig. 7C). There were significant positive temporal and spatial correlations between sham and auditory at all TOIs (Fig. 7C).

The sham-active correlations were stronger than the electric-active correlations between ~60–120 ms and ~150–180 ms, and stronger than the auditory-active correlations between ~130–140 ms (Fig. 8). The sham condition resulted in a larger evoked response compared to the electric condition at all TOIs, and a larger response compared to the auditory condition at the late TOI (Fig. 9).

The summed signal from the electric and auditory conditions showed significant spatial and temporal correlations with the sham condition up until the late TOI, which is where there were relatively fewer temporal correlations and non-significant spatial correlations at ~240 ms (Fig. 10). These findings suggest concurrent somatosensory and auditory stimuli results in a response which is not a simple linear summation of these two inputs, especially at later time-points.

Figs. S1-S8 show the results of all analyses when including ICA in the pre-processing pipeline. Besides differences in the number of GMFW maxima (6 compared to 4) for active TMS and a shift in the early TOI (12–70 instead of 12–55), the overall pattern of results is similar to the main analysis. While the correlations between conditions (Figs. S3 and S5) were less prominent (potentially explained by ICA removing common sensory components), there were still significant positive correlations between active and sham at mid and late TOIs (Fig. S3) and a similar pattern of correlations between active and electric/auditory stimulation (Fig. S5). There was also evidence of stronger potentials (Fig. S7) and stronger correlations with active TMS (Fig. S6) for sham compared to electric/auditory stimulation, and evidence that the sham condition is not a simple linear sum of electrical and auditory stimulation (Fig. S8). These findings suggest that the overall pattern of results is robust even when including ICA in the pre-processing pipeline.

4. Discussion

The first aim of the study was to determine the extent to which auditory and somatosensory-evoked potentials contaminate TEPs when using a spatially matched sham condition. Active TMS generated larger responses than sham between 12–55 ms post-TMS. There were positive spatial and temporal correlations between

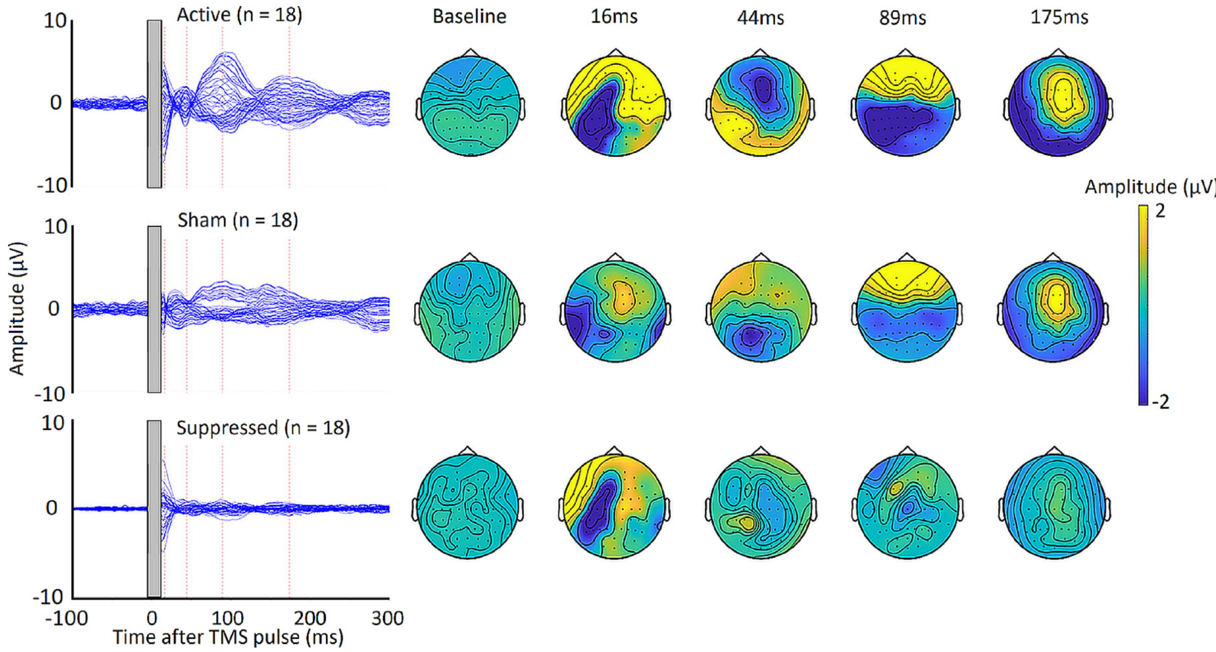

Fig. 4. Transcranial Magnetic Stimulation-evoked potentials (TEPs) and scalp topographies following active and sham stimulation delivered over the left primary motor cortex for the full sample (n = 18). The grey shaded area represents the window of interpolation around the transcranial magnetic stimulation (TMS) pulse. The red dotted lines represent the time-points of the maxima from the global mean field waveforms of the active TMS condition. The scalp topographies show the distribution of voltage at each of these time-points, and the mean topography during the baseline period.

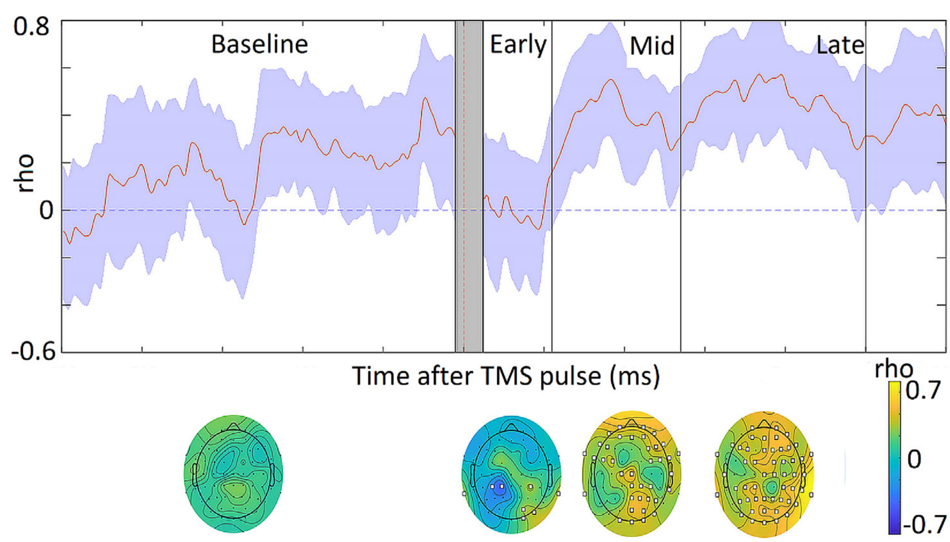

Fig. 5. ***Active and sham signals are correlated at timepoints > 55 ms post-stimulation.*** The figure shows the spatial and temporal correlations between the active and sham conditions. The top panel shows the correlations across electrodes (spatial correlation) between 250 ms before and 300 ms after the Transcranial Magnetic Stimulation (TMS) pulse. The blue shaded area represents the 95% confidence intervals. The grey shaded area represents the window of interpolation around the TMS pulse. The black lines indicate the boundaries for the early (12–55 ms), mid (56–135 ms) and late (136–250 ms) time points of interest (TOI). The bottom panel shows heat maps of the correlations across time (temporal correlation) at each electrode, separated by TOI (early, middle or late) and during the baseline period. The white squares indicate the electrodes with significant correlations (p <.05).

active and sham signals at timepoints > 55 ms. The second aim of the study was to determine how much this contamination was explained by somatosensory or auditory potentials, or a combination of both. Relative to electrical and auditory stimulation alone, the combination of auditory and electrical stimulation (i.e., sham) resulted in a) larger evoked potentials, b) stronger correlations with active TMS and c) a signal that could not be explained by a linear sum of electrical and auditory stimulation.

4.1. Sensory contributions to TMS-evoked potentials

A major focus of current TMS-EEG research has been understanding how sensory-evoked potentials contaminate TEPs. Studies using sham conditions with both sub- and suprathreshold motor cortex stimulation have demonstrated that earlier time-points (<~60 ms post-TMS) are less impacted by sensory contamination (Biabani et al., 2019; Gordon et al., 2018; Poorganji et al.,

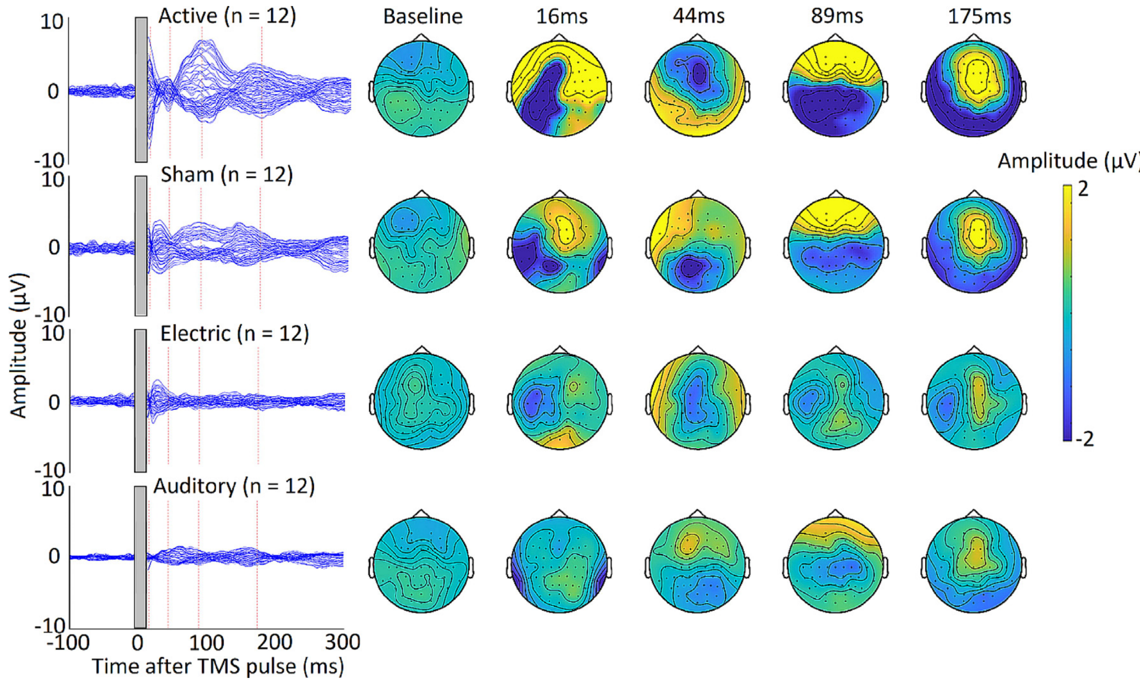

Fig. 6. Transcranial Magnetic Stimulation-evoked potentials (TEPs) and scalp topographies following active, sham, electric and auditory stimulation delivered over the left primary motor cortex (n = 12). The grey shaded area represents the window of interpolation around the TMS pulse. The red dotted lines represent the time-points of the maxima from the global mean field waveforms of the active condition. The scalp topographies show the distribution of voltage at each of these time-points, and the mean topography during the baseline period.

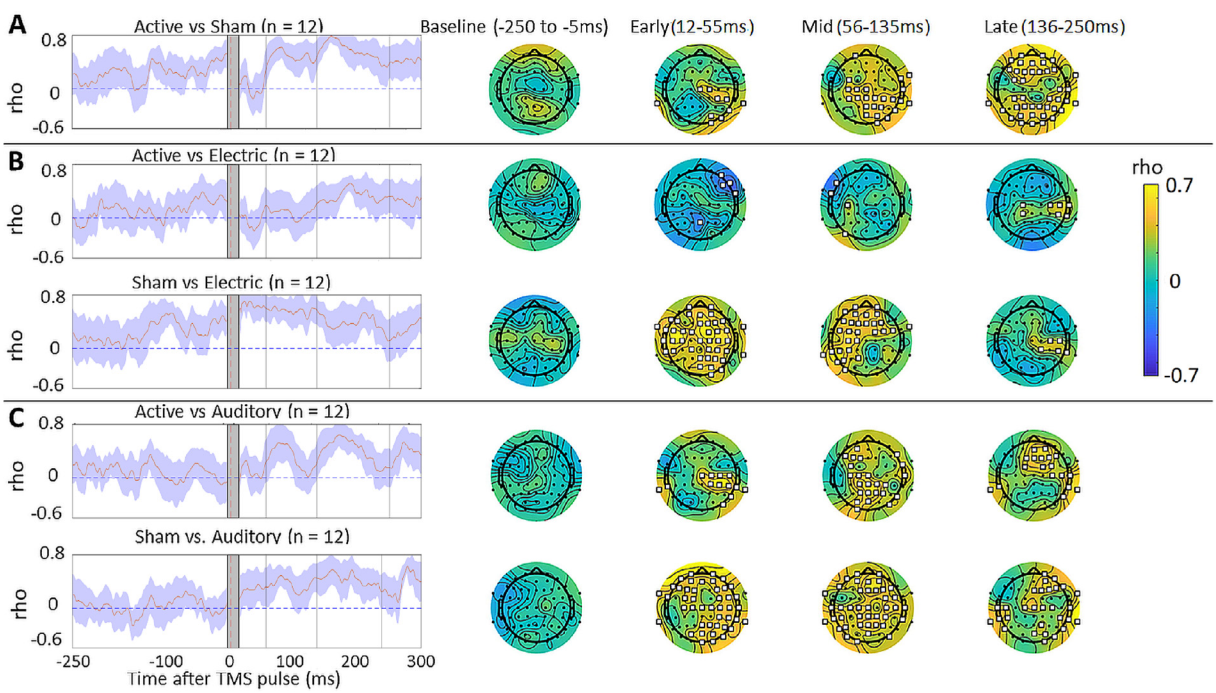

Fig. 7. ***The active and auditory stimulation conditions are correlated at all timepoints of interest, while the active and electrical stimulation conditions are correlated only at late timepoints.*** The figure shows the spatial and temporal correlations for active vs. sham stimulation (panel A), active vs. electrical stimulation and sham vs. electrical stimulation (panel B) and; active vs. auditory stimulation and sham vs. auditory stimulation (panel C). The left panel shows the correlations across electrodes (spatial correlation) between 250 ms before and 300 ms after the TMS pulse. The blue shaded area represents 95% confidence intervals. The vertical black lines indicate the boundaries of the early (12–55 ms), mid (56–135 ms) and late (136–250 ms) time points of interest (TOI). The grey shaded area represents the window of interpolation around the transcranial magnetic stimulation (TMS) pulse. The right panel shows the topography maps demonstrating correlations across time (temporal correlation) at each electrode, separated by TOI (early, middle or late) and during the baseline period. The white squares indicate the electrodes with significant correlations (p <.05).

2021; Rocchi et al., 2021). However, the sensory aspects of most shams were not spatially matched to active TMS. In the current study, the use of a spatially-matched sham did not alter previous findings. Specifically, the amplitude of sensory-evoked potentials was significantly smaller than the active signal at earlier timepoints < 55 ms post-TMS. Moreover, when comparing active

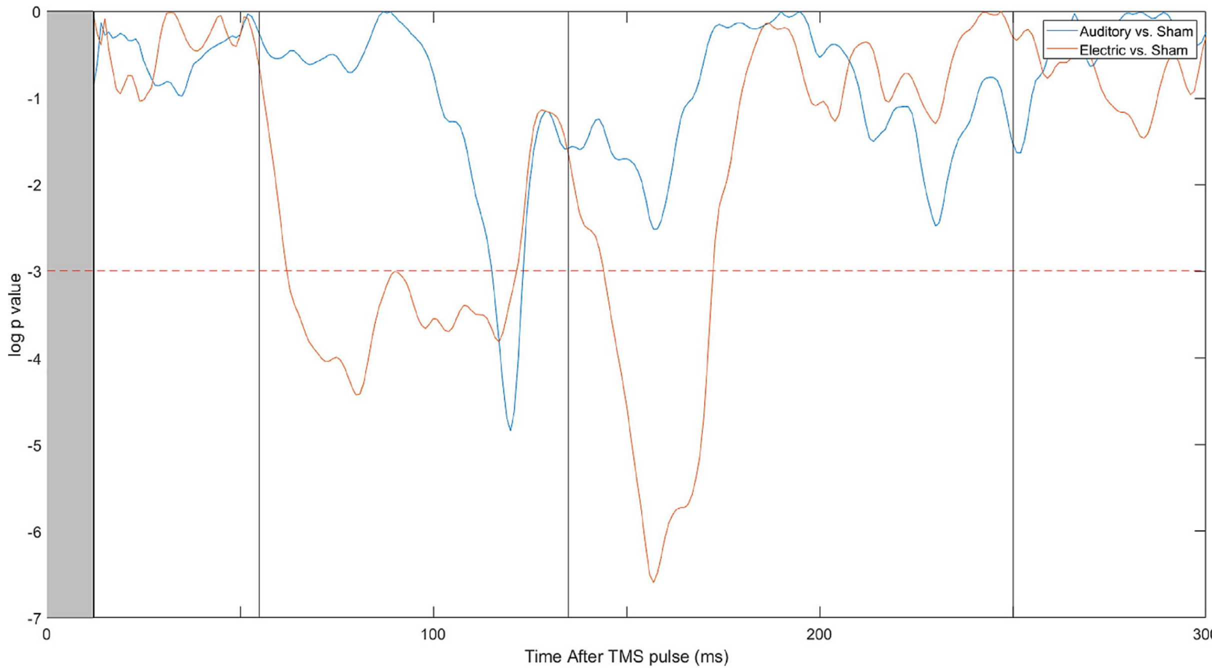

Fig. 8. ***The combination of auditory and electrical stimulation (i.e., the 'sham' condition) is more strongly correlated with active stimulation than auditory or electrical stimulation alone.*** The figure shows the p-values following two-sample t-tests comparing the difference between the sham-active correlation with the auditory-active correlations (blue) and the electric-active correlations (orange). The vertical black lines indicate the boundaries of the early (12–55 ms), mid (56–135 ms) and late (136–250 ms) time points of interest. The grey shaded area represents the window of interpolation around the TMS pulse. The horizontal red dotted line shows the criteria for significance (p =.05). p-values were log-transformed for illustrative purposes.

and sham at these earlier time-points, there were no spatial correlations, and temporal correlations existed at right occipital sites only. This replicates previous findings and support the notion that early timepoints ~<60 ms post-TMS represent the cortical response to TMS. While it is still unknown precisely what mechanisms the early TEP peaks represent, pharmacological studies (Darmani and Ziemann, 2019) and studies comparing TEPs with single and paired-pulse MEPs (Bonato et al., 2006; Komssi et al., 2004; Mäki and Ilmoniemi, 2010) suggest early TEPs may reflect the excitability of the cortex, especially close to the site of stimulation.

An important finding was evidence of perceptual matching between active and sham conditions, particularly for the somatosensory ratings (flick sharpness and strength). Matching the perceptual aspects of active and sham stimulation has been a major challenge in previous studies (Biabani et al., 2019; Conde et al., 2019; Gordon et al., 2021). However, most studies used sham conditions where active TMS was delivered at a distance from the scalp (Biabani et al., 2019; Conde et al., 2019; Gordon et al., 2018). A recent study (Gordon et al., 2021) achieved perceptual matching by delivering high intensity electrical stimulation in both active and sham conditions to render both indistinguishable. Though this was effective in blinding participants, the inclusion of electrical stimulation in the active condition may have altered the genuine TEP response. This highlights one advantage of the current setup as somatosensory ratings were matched without the need for electrical stimulation during active TMS. However, a more thorough assessment is required to determine whether the sham stimuli in the present study is indistinguishable from active TMS.

4.2. Individual sensory contributions to TMS-evoked potentials

The findings align with previous work showing auditory potentials make a greater contribution to TEPs when compared with somatosensory potentials (Rocchi et al., 2021). However, the present study also showed the amplitude of the combined response to electrical and auditory stimulation (i.e., the sham) was larger than for either electrical or auditory stimulation alone, resulting in stronger correlations with the active condition at late TOIs. Combined stimulation was also perceptually rated as providing stronger brain stimulation. Furthermore, summating the responses from the auditory and electrical conditions did not recover the combined EEG response at late TOIs, suggesting the concurrent input of the two sensory stimuli results in a non-linear interaction within the brain. Some authors have used sham conditions consisting of only auditory stimuli (Poorganji et al., 2021), and others have concluded that controlling for auditory potentials alone may be sufficient to index excitability (Rocchi et al., 2021). The present findings suggest even though somatosensory contributions to TEPs are smaller than auditory contributions, sensory contamination of TEPs is best explained as a non-linear interaction between somatosensory and auditory inputs. Together, these findings suggest sham conditions using concurrent auditory and somatosensory stimuli can more accurately capture sensory contamination within TEPs, and more closely match the perceptual experience of active TMS.

4.3. Limitations

There are several limitations to discuss. First, the electrical stimulation used in the sham condition, although well matched to the active condition in terms of flick strength and sharpness, did not induce the facial/cranial nerve stimulation which may be associated with active TMS (Mutanen et al., 2013; Rogasch and Fitzgerald, 2013). This could explain the more prominent contribution of auditory stimulation in the active, relative to the sham, condition. Another limitation may be the absence of auditory noise masking. Indeed, a recent study (Rocchi et al., 2021) showed mixing white noise with specific time-varying frequencies of the TMS click through headphones results in a significantly smaller auditory

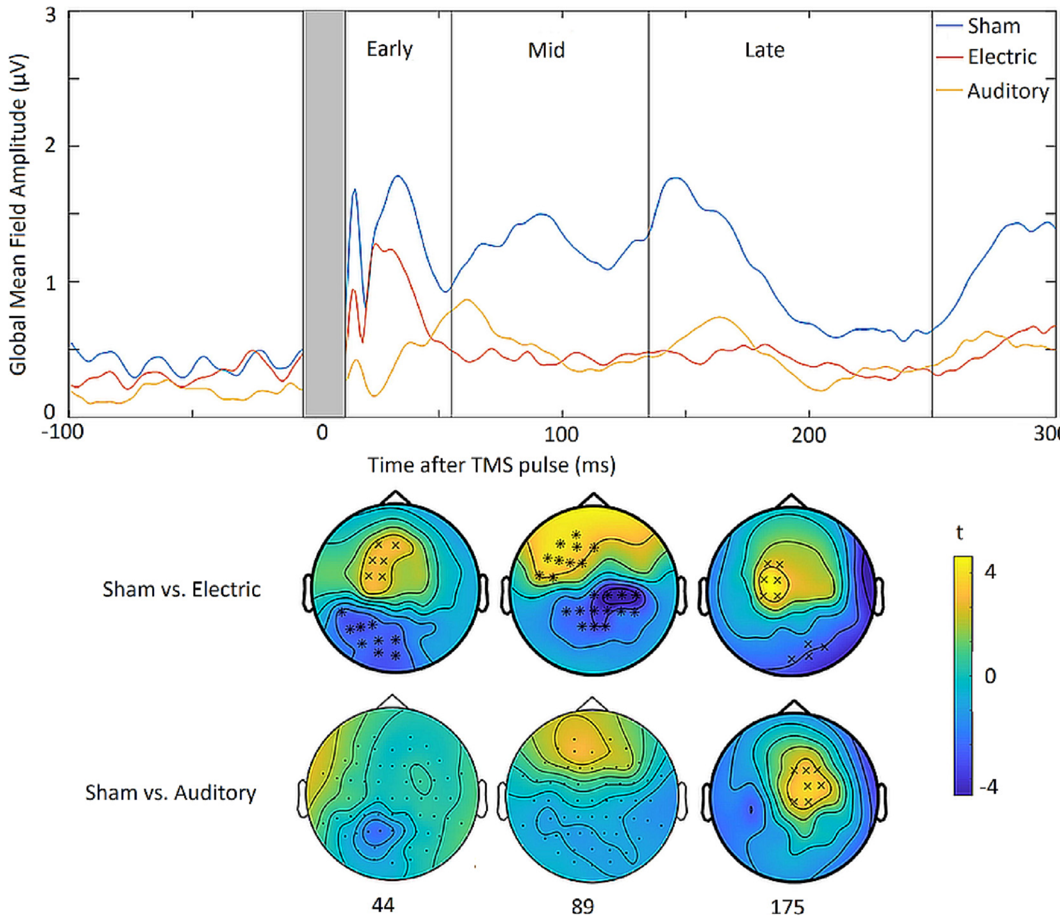

Fig. 9. ***The combination of auditory and electrical stimulation (i.e., the 'sham' condition) results in larger evoked potentials than auditory or electrical stimulation alone***. The figure shows the amplitude comparisons between the combined auditory and electrical (sham), electric alone and auditory alone signals. The top panel shows the global mean field waveforms for the three conditions. The black solid lines represent the boundaries of the time points of interest (TOI)– early (12–55 ms), mid (56–135 ms) and late (136–250 ms). The bottom panel shows the cluster plots comparing signal amplitude between sham, electrical and auditory stimulation at a representative time-point within each TOI (early –44 ms, mid –89 ms and late –175 ms). The black stars denote the presence of significant positive (yellow) or negative (blue) clusters.

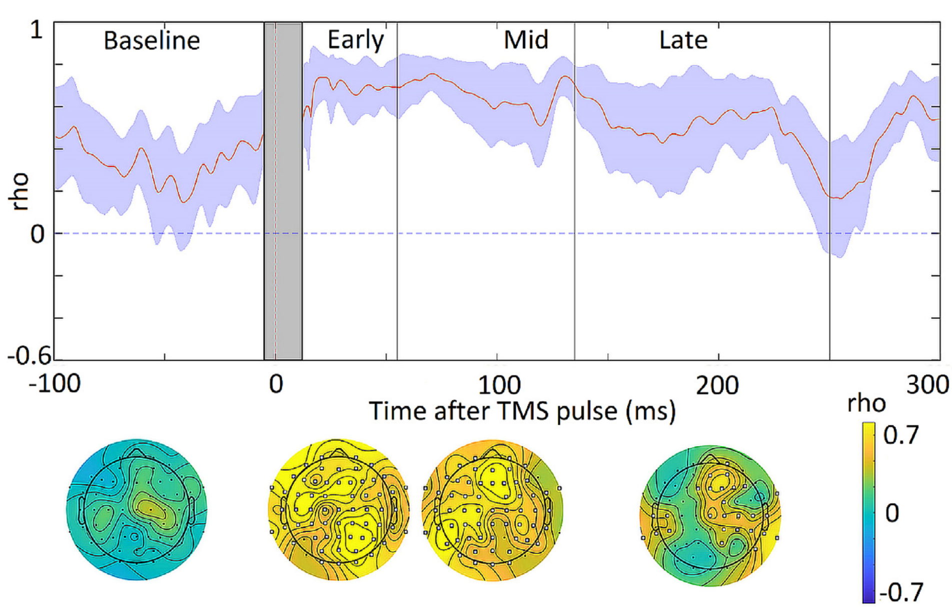

Fig. 10. ***The combination of auditory and electrical stimulation (i.e., the 'sham' condition) resulted in a signal that could not be explained by the linear sum of the electrical alone and auditory alone signals***. The figure shows the spatial and temporal correlations between the sham condition and the summed potential of the electrical and auditory alone conditions auditory alone and electric alone conditions. The blue shaded area represents 95% confidence intervals. The grey shaded area represents the window of interpolation around the transcranial magnetic stimulation (TMS) pulse. The top panel shows the correlations across electrodes (spatial correlation) between 250 ms before and 300 ms after the TMS pulse. The vertical black lines indicate the boundaries of the early (12–55 ms), mid (56–135 ms) and late (136–250 ms) timepoints of interest (TOIs). The bottom panel shows heat maps of the correlations across time (temporal correlation) at each electrode, separated by TOI (early, middle or late) and during the baseline period. The white squares indicate the electrodes with significant correlations (p <.05).

response. However, as the goal of our study was to assess correlations between the auditory click of sham TMS with active TMS, and to compare loudness ratings between active and sham, we did not opt for complete auditory suppression. Finally, reafferent activity from the motor-evoked response in peripheral muscles can also alter TEPs (Biabani et al., 2021; Fecchio et al., 2017; Pellicciari et al., 2017), and may explain the absence of early correlations between active and sham. This was not controlled for in the current study. Further studies are required comparing the signals produced by active and sham stimulation in the presence of auditory masking, as well as using somatosensory stimulation which activates cranial nerves.

4.4. Conclusions

The present findings replicate previous studies showing sensory potentials can significantly contaminate EEG signals at timepoints $\sim$>55 ms post-stimulation. Further, the findings provide evidence that concurrent auditory and somatosensory input can capture sensory contamination more accurately than auditory or somatosensory input alone. Future TMS-EEG studies may benefit from controlling for sensory contamination using sham conditions that are spatially matched to active TMS and consist of combined auditory and somatosensory stimulation.

Funding source

None.

Author contributions

N.C. was involved in conceptualization, data curation, formal analysis, investigation, methodology, project administration, validation, visualisation, writing – original draft, writing – review and editing. N.R. was involved in supervision, software, conceptualization, formal analysis and writing – review and editing. A.C. was involved in conceptualization, formal analysis and writing – review and editing S.M. was involved in conceptualization, formal analysis and writing – review and editing. P.S., K.B., and E.S. were involved in writing – review and editing. D.S. was involved in resources, supervision and writing – review and editing. S.M. was involved in resources, supervision and writing – review and editing.

Declaration of Competing Interest

The authors declare that they have no known competing financial interests or personal relationships that could have appeared to influence the work reported in this paper.

Appendix A. Supplementary material

Supplementary data to this article can be found online at https://doi.org/10.1016/j.clinph.2022.05.015.s

References

Arana AB, Borckardt JJ, Ricci R, Anderson B, Li X, Linder KJ, et al. Focal electrical stimulation as a sham control for repetitive transcranial magnetic stimulation: Does it truly mimic the cutaneous sensation and pain of active prefrontal repetitive transcranial magnetic stimulation? Brain Stimul 2008;1(1):44–51. https://doi.org/10.1016/j.brs.2007.08.006.

Awiszus F, Borckardt J. TMS motor threshold assessment tool (MTAT 2.0). Brain Stimulation Laboratory, Medical University of South Carolina, USA; 2011. Available at: http://www.clinicalresearcher.org/software.htm.

Biabani M, Fornito A, Coxon JP, Fulcher BD, Rogasch NC. The correspondence between EMG and EEG measures of changes in cortical excitability following transcranial magnetic stimulation. J Physiol 2021;599(11):2907–32.

Biabani M, Fornito A, Mutanen TP, Morrow J, Rogasch NC. Characterizing and minimizing the contribution of sensory inputs to TMS-evoked potentials. Brain Stimul 2019;12(6):1537–52. https://doi.org/10.1016/j.brs.2019.07.009.

Bonato C, Miniussi C, Rossini P. Transcranial magnetic stimulation and cortical evoked potentials: a TMS/EEG co-registration study. Clin Neurophysiol 2006;117(8):1699–707. https://doi.org/10.1016/j.clinph.2006.05.006.

Calvert GA, Campbell R, Brammer MJ. Evidence from functional magnetic resonance imaging of crossmodal binding in the human heteromodal cortex. Curr Biol 2000;10(11):649–57. https://doi.org/10.1016/S0960-9822(00)00513-3.

Calvert GA, Hansen PC, Iversen SD, Brammer MJ. Detection of audio-visual integration sites in humans by application of electrophysiological criteria to the BOLD effect. Neuroimage 2001;14(2):427–38. https://doi.org/10.1006/nimg.2001.0812.

Casula EP, Rocchi L, Hannah R, Rothwell JC. Effects of pulse width, waveform and current direction in the cortex: A combined cTMS-EEG study. Brain Stimul 2018;11(5):1063–70. https://doi.org/10.1016/j.brs.2018.04.015.

Conde V, Tomasevic L, Akopian I, Stanek K, Saturnino GB, Thielscher A, Bergmann TO, Siebner HR. The non-transcranial TMS-evoked potential is an inherent source of ambiguity in TMS-EEG studies. Neuroimage 2019;185:300–12. https://doi.org/10.1016/j.neuroimage.2018.10.052.

Darmani G, Ziemann U. Pharmacophysiology of TMS-evoked EEG potentials: a mini-review. Brain Stimul 2019;12(3):829–31. https://doi.org/10.1016/j.brs.2019.02.021.

Delorme A, Makeig S. EEGLAB: an open source toolbox for analysis of single-trial EEG dynamics including independent component analysis. J Neurosci Methods 2004;134(1):9–21. https://doi.org/10.1016/j.jneumeth.2003.10.009.

Delorme A, Sejnowski T, Makeig S. Enhanced detection of artifacts in EEG data using higher-order statistics and independent component analysis. Neuroimage 2007;34(4):1443–9. https://doi.org/10.1016/j.neuroimage.2006.11.004.

Farzan F, Vernet M, Shafi M, Rotenberg A, Daskalakis ZJ, Pascual-Leone A. Characterizing and modulating brain circuitry through transcranial magnetic stimulation combined with electroencephalography. Front Neural Circuits 2016;10:73. https://doi.org/10.3389/fncir.2016.00073.

Fecchio M, Pigorini A, Comanducci A, Sarasso S, Casarotto S, Premoli I, Derchi C-C, Mazza A, Russo S, Resta F. The spectral features of EEG responses to transcranial magnetic stimulation of the primary motor cortex depend on the amplitude of the motor evoked potentials. PLoS ONE 2017;12(9):e0184910. https://doi.org/10.1371/journal.pone.0184910.

Fernandez L, Biabani M, Do M, Opie GM, Hill AT, Barham MP, Teo W-P, Byrne LK, Rogasch NC, Enticott PG. Assessing cerebellar-cortical connectivity using concurrent TMS-EEG: a feasibility study. J Neurophysiol 2021;125(5):1768–87. https://doi.org/10.1152/jn.00617.2020.

Gordon PC, Desideri D, Belardinelli P, Zrenner C, Ziemann U. Comparison of cortical EEG responses to realistic sham versus real TMS of human motor cortex. Brain Stimul 2018;11(6):1322–30. https://doi.org/10.1016/j.brs.2018.08.003.

Gordon PC, Jovellar DB, Song Y, Zrenner C, Belardinelli P, Siebner HR, Ziemann U. Recording brain responses to TMS of primary motor cortex by EEG–utility of an optimized sham procedure. Neuroimage 2021;245:118708. https://doi.org/10.1016/j.neuroimage.2021.118708.

Ilmoniemi RJ, Kičić DJBT. Methodology for combined TMS and EEG. Brain Topogr 2010;22(4):233–48. https://doi.org/10.1007/s10548-009-0123-4.

Kerwin LJ, Keller CJ, Wu W, Narayan M, Etkin A. Test-retest reliability of transcranial magnetic stimulation EEG evoked potentials. Brain Stimul 2018;11(3):536–44. https://doi.org/10.1016/j.brs.2017.12.010.

Kičić D. Probing cortical excitability with transcranial magnetic stimulation. Ph.D. Thesis. Helsinki University of Technology, Espoo; 2009. Available at: http://urn.fi/URN:ISBN:978-952-248-057-6.

Komssi S, Kähkönen S, Ilmoniemi RJ. The effect of stimulus intensity on brain responses evoked by transcranial magnetic stimulation. Hum Brain Mapp 2004;21(3):154–64. https://doi.org/10.1002/hbm.10159.

Lippert MT, Takagaki K, Kayser C, Ohl FW, Maravall M. Asymmetric multisensory interactions of visual and somatosensory responses in a region of the rat parietal cortex. PLoS ONE 2013;8(5):e63631. https://doi.org/10.1371/journal.pone.0063631.

Mäki H, Ilmoniemi RJ. The relationship between peripheral and early cortical activation induced by transcranial magnetic stimulation. Neurosci Lett 2010;478(1):24–8. https://doi.org/10.1016/j.neulet.2010.04.059.

Mancuso M, Sveva V, Cruciani A, Brown K, Ibáñez J, Rawji V, Casula E, Premoli I, D'Ambrosio S, Rothwell J, Rocchi L. Transcranial evoked potentials can be reliably recorded with active electrodes. Brain Sci 2021;11(2):145. https://doi.org/10.3390/brainsci11020145.

Massimini M, Ferrarelli F, Huber R, Esser SK, Singh H, Tononi GJS. Breakdown of cortical effective connectivity during sleep. Science 2005;309(5744):2228–32. https://doi.org/10.1126/science.1117256.

Mutanen T, Mäki H, Ilmoniemi RJ. The effect of stimulus parameters on TMS–EEG muscle artifacts. Brain Stimul 2013;6(3):371–6. https://doi.org/10.1016/j.brs.2012.07.005.

Mutanen TP, Biabani M, Sarvas J, Ilmoniemi RJ, Rogasch NC. Source-based artifact-rejection techniques available in TESA, an open-source TMS–EEG toolbox. Brain Stimul 2020;13(5):1349–51. https://doi.org/10.1016/j.brs.2020.06.079.

Mutanen TP, Metsomaa J, Liljander S, Ilmoniemi RJ. Automatic and robust noise suppression in EEG and MEG: The SOUND algorithm. Neuroimage 2018;166:135–51. https://doi.org/10.1016/j.neuroimage.2017.10.021.

Neumaier A, Schneider T. Estimation of parameters and eigenmodes of multivariate autoregressive models. ACM Trans Math Softw 2001;27(1):27–57. https://doi.org/10.1145/382043.382304.

Nikbakht N, Tafreshiha A, Zoccolan D, Diamond ME. Supralinear and supramodal integration of visual and tactile signals in rats: psychophysics and neuronal mechanisms. Neuron 2018;97(3):626–39. https://doi.org/10.1016/j.neuron.2018.01.003.

Oostenveld R, Fries P, Maris E, Schoffelen J-M. FieldTrip: Open Source Software for Advanced Analysis of MEG, EEG, and Invasive Electrophysiological Data. Comput Intell Neurosci 2011;2011:1–9. https://doi.org/10.1155/2011/156869.

Pellicciari MC, Ponzo V, Caltagirone C, Koch G. Restored asymmetry of prefrontal cortical oscillatory activity after bilateral theta burst stimulation treatment in a patient with major depressive disorder: a TMS-EEG study. Brain Stimul 2017;10(1):147–9. https://doi.org/10.1016/j.brs.2016.09.006.

Poorganji M, Zomorrodi R, Hawco C, Hill AT, Hadas I, Rajji TK, Chen R, Voineskos D, Daskalakis AA, Blumberger DM, Daskalakis ZJ. Differentiating Transcranial Magnetic Stimulation Cortical and Auditory Responses via Single Pulse and Paired Pulse protocols: A TMS-EEG study. Clin Neurophysiol 2021;132(8):1850–8. https://doi.org/10.1016/j.clinph.2021.05.009.

Rocchi L, Di Santo A, Brown K, Ibanez J, Casula E, Rawji V, Di Lazzaro V, Koch G, Rothwell J. Disentangling EEG responses to TMS due to cortical and peripheral activations. Brain Stimul 2021;14(1):4–18. https://doi.org/10.1016/j.brs.2020.10.011.

Rogasch NC, Biabani M, Mutanen TP. Designing and comparing cleaning pipelines for TMS-EEG data: a theoretical overview and practical example. J Neurosci Methods 2022;371:109494. https://doi.org/10.1016/j.jneumeth.2022.109494.

Rogasch NC, Fitzgerald PB. Assessing cortical network properties using TMS–EEG. Hum Brain Mapp 2013;34(7):1652–69. https://doi.org/10.1002/hbm.22016.

Rogasch NC, Sullivan C, Thomson RH, Rose NS, Bailey NW, Fitzgerald PB, Farzan F, Hernandez-Pavon JC. Analysing concurrent transcranial magnetic stimulation and electroencephalographic data: A review and introduction to the open-source TESA software. Neuroimage 2017;147:934–51. https://doi.org/10.1016/j.neuroimage.2016.10.031.

Ronga I, Galigani M, Bruno V, Noel J-P, Gazzin A, Perathoner C, et al. Spatial tuning of electrophysiological responses to multisensory stimuli reveals a primitive coding of the body boundaries in newborns. Proc Natl Acad Sci U S A 2021;118(12). https://doi.org/10.1073/pnas.2024548118.

Rossi S, Hallett M, Rossini PM, Pascual-Leone A. Safety, ethical considerations, and application guidelines for the use of transcranial magnetic stimulation in clinical practice and research. Clin Neurophysiol 2009;120(12):2008–39. https://doi.org/10.1016/j.clinph.2009.08.016.

Rossini PM, Barker AT, Berardelli A, Caramia MD, Caruso G, Cracco RQ, et al. Non-invasive electrical and magnetic stimulation of the brain, spinal cord and roots: basic principles and procedures for routine clinical application. Report of an IFCN committee. Electroencephalogr Clin Neurophysiol 1994;91(2):79–92. https://doi.org/10.1016/0013-4694(94)90029-9.

Rothwell JC, Hallett M, Berardelli A, Eisen A, Rossini P, Paulus W. Magnetic stimulation: motor evoked potentials. The International Federation of Clinical Neurophysiology. Electroencephalogr Clin Neurophysiol Supplement 1999;52:97–103.

Schneider T, Neumaier A. Algorithm 808: ARfit—A Matlab package for the estimation of parameters and eigenmodes of multivariate autoregressive models. ACM Trans Math Softw 2001;27(1):58–65. https://doi.org/10.1145/382043.382316.

Sekiguchi H, Takeuchi S, Kadota H, Kohno Y, Nakajima Y. TMS-induced artifacts on EEG can be reduced by rearrangement of the electrode's lead wire before recording. Clin Neurophysiol 2011;122(5):984–90. https://doi.org/10.1016/j.clinph.2010.09.004.

Senkowski D, Gomez-Ramirez M, Lakatos P, Wylie GR, Molholm S, Schroeder CE, Foxe JJ. Multisensory processing and oscillatory activity: analyzing non-linear electrophysiological measures in humans and simians. Exp Brain Res 2007;177(2):184–95. https://doi.org/10.1007/s00221-006-0664-7.

Smith JE, Peterchev AV. Electric field measurement of two commercial active/sham coils for transcranial magnetic stimulation. J Neural Eng 2018;15(5):054001. https://doi.org/10.1088/1741-2552/aace89.

Stefan AM, Gronau QF, Schönbrodt FD, Wagenmakers E-J. A tutorial on Bayes Factor Design Analysis using an informed prior. Behav Res Methods 2019;51(3):1042–58. https://doi.org/10.3758/s13428-018-01189-8.

Tremblay S, Rogasch NC, Premoli I, Blumberger DM, Casarotto S, Chen R, et al. Clinical utility and prospective of TMS–EEG. Clinical utility and prospective of TMS–EEG. Clin Neurophysiol 2019;130(5):802–44. https://doi.org/10.1016/j.clinph.2019.01.001.